

Linear viscoelasticity of semidilute hard-sphere suspensions

B. Cichocki*

Institute of Theoretical Physics, Warsaw University, Hoza 69, 00-681 Warsaw, Poland

B. U. Felderhof

Institut für Theoretische Physik A, Rheinisch-Westfälische Technische Hochschule Aachen, Templergraben 55, 5100 Aachen, Germany

(Received 16 October 1990)

We study the linear viscoelasticity of semidilute suspensions of spherical Brownian particles. We consider a simple model in which hydrodynamic interactions and direct interactions apart from hard-sphere repulsion are neglected. We calculate the dynamic viscosity for this model system exactly to second order in the volume fraction. It turns out that the infinite-frequency shear modulus does not exist because the dynamic viscosity falls off with the inverse square root of the frequency. The relaxation-rate spectrum has corresponding inverse-square-root behavior. We find exact expressions for the spectral density and the time-dependent stress-relaxation function. Qualitatively our results resemble those found experimentally for dense hard-sphere suspensions.

I. INTRODUCTION

Dilute polymer solutions exhibit a marked viscoelasticity due to the flexibility of the individual polymer molecules.¹ In the linear regime the viscoelasticity is manifested in the frequency dependence of the shear viscosity. The viscosity of a dilute suspension of rigid hard spheres does not depend on frequency, and is given by the Einstein expression.² However, at higher concentrations, the viscosity becomes frequency dependent due to relaxation of the relative configuration.³ The effect has been measured experimentally by van der Werff *et al.*⁴ for dense suspensions with volume fractions between 0.3 and 0.6. They found an interesting inverse-square-root dependence on frequency. This indicates a broad spectrum of relaxation times, similar to that for the Rouse model of dilute polymer solutions.⁵ Earlier measurements by Mellema *et al.*⁶ were explained in terms of a single relaxation time.

In this article we study a simple model of a hard-sphere suspension in which hydrodynamic interactions and direct interactions, besides the hard-sphere repulsion, are neglected. We calculate the dynamic viscosity exactly to second order in the volume fraction and show that the asymptotic dependence on frequency is similar to that found in the experiments by van der Werff *et al.*⁴

We also discuss an excluded shell model with a radius of hard-sphere repulsion larger than the hydrodynamic radius. The dynamic viscosity for this model may be obtained from that for the hard-sphere model by simple scaling. The model may give a fairly realistic picture of the behavior of suspensions of charged polystyrene spheres. For such suspensions, hydrodynamic interactions are relatively unimportant, since these are determined by the actual hard core radius, whereas the spheres are kept apart by electrostatic interactions. The resulting structure resembles that of a hard-sphere system with an effective radius equal to the actual one plus the

Debye length. If the latter is sufficiently large, the hydrodynamic interactions are small.

II. LINEAR VISCOELASTICITY

We consider a spatially uniform suspension subjected to an oscillating shear flow with time dependence $\exp(-i\omega t)$. For small-amplitude oscillations, the local stress and rate of strain are related by a frequency-dependent viscosity $\eta(\omega)$. The imaginary part of the dynamic viscosity

$$\eta(\omega) = \eta'(\omega) + i\eta''(\omega) \quad (2.1)$$

is related to the dynamic shear modulus $G(\omega)$ by

$$G(\omega) = -i\omega\eta(\omega) = G'(\omega) - iG''(\omega). \quad (2.2)$$

The infinite-frequency value $G_\infty = G'(\infty)$ is called the high-frequency modulus.

In the simplest model, due to Maxwell, the dynamic viscosity is characterized by a single relaxation time and takes the form

$$\eta(\omega) = \eta_\infty + \frac{G_\infty \tau}{1 - i\omega\tau}. \quad (2.3)$$

More generally, one must consider a spectrum of relaxation times and write the dynamic viscosity as

$$\eta(\omega) = \eta_\infty + G_\infty \int_0^\infty \frac{\tau P(\tau)}{1 - i\omega\tau} d\tau, \quad (2.4)$$

where $P(\tau)$ is the normalized distribution of relaxation times.⁷ It is convenient to introduce a characteristic time scale τ_0 . In dimensionless units we may then write (2.4) in the form

$$\eta(\omega) = \eta_\infty + G_\infty \tau_0 \int_0^\infty \frac{\sigma \hat{P}(\sigma)}{1 - i\hat{\omega}\sigma} d\sigma, \quad (2.5)$$

with the dimensionless relaxation time $\sigma = \tau/\tau_0$, the di-

dimensionless frequency $\hat{\omega} = \omega\tau_0$, and with normalization

$$\int_0^\infty \hat{P}(\sigma) d\sigma = 1. \quad (2.6)$$

Alternatively, we may use a distribution of relaxation rates and write

$$\eta(\omega) = \eta_\infty + G_\infty \tau_0 \int_0^\infty \frac{p(u)}{u-z} du, \quad (2.7)$$

with the variables

$$u = \frac{1}{\sigma} = \frac{\tau_0}{\tau}, \quad z = i\hat{\omega} = i\omega\tau_0, \quad (2.8)$$

and distribution function

$$p(u) = \hat{P}(1/u)/u^2, \quad (2.9)$$

which is normalized to unity

$$\int_0^\infty p(u) du = 1. \quad (2.10)$$

The mean relaxation time τ_m is given by

$$\tau_m = \tau_0 \int_0^\infty \sigma \hat{P}(\sigma) d\sigma = \tau_0 \int_0^\infty \frac{1}{u} p(u) du. \quad (2.11)$$

The dynamic viscosity may also be expressed as the one-sided Fourier transform of the stress-relaxation function

$$\eta(\omega) = \eta_\infty + \frac{\eta}{\tau_0} \int_0^\infty e^{i\omega t} \Psi(t) dt, \quad (2.12)$$

where η is the viscosity of the solvent. By comparison with (2.7) we find that the relaxation function may be regarded as a linear superposition of decaying exponentials

$$\Psi(t) = \frac{G_\infty \tau_0}{\eta} \int_0^\infty p(u) \exp\left[-\frac{ut}{\tau_0}\right] du. \quad (2.13)$$

The long-time behavior of the relaxation function is dominated by the behavior of the spectral function at small u .

In the following, we encounter a situation where the high-frequency modulus G_∞ is not defined, because the dynamic modulus $G'(\omega)$ does not tend to a limit at infinite frequency. In analogy to (2.7) we write the dynamic viscosity as

$$\eta(\omega) = \eta_\infty + G_v \tau_0 \int_0^\infty \frac{p(u)}{u-z} du. \quad (2.14)$$

We consider the situation, where the spectrum has the asymptotic behavior

$$p(u) \approx \frac{1}{\mu} u^{-1+1/\mu} \quad \text{as } u \rightarrow \infty \quad (2.15)$$

with exponent $\mu > 1$. The spectral density $p(u)$ can no longer be regarded as a probability distribution, since the normalization integral in (2.10) diverges. We call G_v the relaxation strength.

It follows from (2.14) and (2.15) that the asymptotic behavior for large ω of the real part of the dynamic viscosity is given by

$$\eta'(\omega) \approx \eta_\infty + \frac{\pi}{2\mu \cos(\pi/2\mu)} G_v \tau_0 \hat{\omega}^{-1+1/\mu} \quad \text{as } \omega \rightarrow \infty. \quad (2.16)$$

Correspondingly, the asymptotic behavior of the imaginary part is given by

$$\eta''(\omega) \approx \frac{\pi}{2\mu \sin(\pi/2\mu)} G_v \tau_0 \hat{\omega}^{-1+1/\mu} \quad \text{as } \omega \rightarrow \infty. \quad (2.17)$$

Asymptotic behavior of the form (2.16) and (2.17) has been found for dilute polymer solutions.^{5,8} The exponent μ takes the value 2 in the Rouse model.

III. VISCOSITY OF HARD-SPHERE SUSPENSIONS

We study specifically the dynamic viscosity of a suspension of hard spheres. We consider identical hard spheres of radius a immersed in an incompressible fluid of shear viscosity η . We neglect hydrodynamic interactions and assume that each sphere performs Brownian motion with a bare diffusion coefficient D_0 given by the Stokes-Einstein expression $k_B T/6\pi\eta a$. We also assume that there is no direct interaction besides the hard-sphere repulsion at diameter $2a$. We consider a macroscopically uniform system of mean number density n . Due to the neglect of hydrodynamic interaction, the infinite-frequency value of the viscosity is given by the Einstein expression²

$$\eta_\infty = \eta(1 + \frac{5}{2}\phi), \quad (3.1)$$

where $\phi = 4\pi n a^3/3$ is the volume fraction occupied by spheres.

On the time scale seen in light-scattering experiments, the dynamics of the system of interacting Brownian particles is governed by the generalized Smoluchowski equation⁹ incorporating independent diffusion and hard-sphere repulsion. The dynamic viscosity may be calculated by applying linear-response theory to the Smoluchowski equation.¹⁰ To second order in the volume fraction, one finds^{3,11}

$$\eta(\omega) = \eta_\infty + \alpha_V(\omega) \phi^2 \eta, \quad (3.2)$$

with a dimensionless coefficient $\alpha_V(\omega)$ which may be evaluated from a solution of the two-sphere Smoluchowski equation. In an imposed oscillatory shear flow $\mathbf{v}_{0\omega}(\mathbf{r}) = \mathbf{E}_\omega \cdot \mathbf{r}$, with rate of strain tensor \mathbf{E}_ω , the perturbation of the pair-distribution function takes the form

$$\delta P(\mathbf{R}, \omega) = -3\pi\beta\eta a^3 n^2 \mathbf{E}_\omega : \hat{\mathbf{R}} \hat{\mathbf{R}} g(R) f(x, \omega), \quad (3.3)$$

where $\mathbf{R} = \mathbf{R}_2 - \mathbf{R}_1$ is the distance between centers of a pair of spheres, $\beta = 1/k_B T$, and $g(R)$ is the equilibrium radial distribution function. The radial function $f(x, \omega)$ is expressed in terms of the dimensionless variable $x = R/2a$. For a dilute system of hard spheres, $g(R) = \Theta(R - 2a)$, where Θ is the step function. With neglect of hydrodynamic interactions, the coefficient in (3.2) is given by the simple expression.

$$\alpha_V(\omega) = \frac{2}{3} f(1, \omega). \quad (3.4)$$

The radial function $f(x, \omega)$ satisfies the differential equation

$$\frac{d}{dx} \left[x^2 \frac{df}{dx} \right] - 6f - \alpha^2 x^2 f = 0, \quad (3.5)$$

where for positive ω

$$\alpha = (1-i)(\omega a^2/D_0)^{1/2}. \quad (3.6)$$

The differential equation must be solved subject to the boundary conditions¹²

$$f'(1) = -4, \quad f \rightarrow 0 \quad \text{as } x \rightarrow \infty. \quad (3.7)$$

The first condition expresses the hard-sphere repulsion.

The solution of (3.5) with the boundary conditions (3.7) is given by

$$f(x, \omega) = -\frac{4}{\alpha k_2'(\alpha)} k_2(\alpha x), \quad (3.8)$$

where $k_2(z)$ is a modified spherical Bessel function. Substituting in (3.4) we find

$$\alpha_V(\omega) = \frac{36}{5} \frac{\alpha^2 + 3\alpha + 3}{\alpha^3 + 4\alpha^2 + 9\alpha + 9}. \quad (3.9)$$

In the present problem it is natural to use the time scale $\tau_0 = a^2/D_0$. Correspondingly, we define the dimensionless frequency

$$\hat{\omega} = \omega \tau_0, \quad \tau_0 = a^2/D_0. \quad (3.10)$$

For positive ω , we find for the real and imaginary parts of the dynamic viscosity

$$\begin{aligned} \eta'(\omega) &= \eta_\infty + \frac{36}{5} \frac{AC + BD}{C^2 + D^2} \phi^2 \eta, \\ \eta''(\omega) &= \frac{36}{5} \frac{AD - BC}{C^2 + D^2} \phi^2 \eta, \end{aligned} \quad (3.11)$$

with the abbreviations

$$\begin{aligned} A &= 3 + 3(\hat{\omega})^{1/2}, \quad B = 2\hat{\omega} + 3(\hat{\omega})^{1/2}, \\ C &= -2\hat{\omega}^{3/2} + 9(\hat{\omega})^{1/2} + 9, \quad D = 2\hat{\omega}^{3/2} + 8\hat{\omega} + 9. \end{aligned} \quad (3.12)$$

For negative ω , the viscosity follows from the symmetry

$$\eta'(-\omega) = \eta'(\omega), \quad \eta''(-\omega) = -\eta''(\omega). \quad (3.13)$$

At zero frequency,

$$\alpha_V(0) = \frac{12}{5}. \quad (3.14)$$

This result was found earlier by Russel.¹³ For large positive frequency,

$$\begin{aligned} \eta'(\omega) &\approx \eta_\infty + \frac{18}{5} \frac{\phi^2}{\sqrt{\omega \tau_0}} \eta, \\ \eta''(\omega) &\approx \frac{18}{5} \frac{\phi^2}{\sqrt{\omega \tau_0}} \eta \quad \text{as } \omega \rightarrow \infty. \end{aligned} \quad (3.15)$$

This shows that the viscoelastic spectrum is of the power-law type with exponent $\mu = 2$. By comparison with (2.16) and (2.17) we find for the relaxation strength

$$G_v = \frac{36\sqrt{2}}{5\pi} \phi^2 \frac{\eta}{\tau_0}. \quad (3.16)$$

It is of interest to introduce the reduced functions

$$\begin{aligned} R(\omega) &\equiv \frac{\eta'(\omega) - \eta_\infty}{\eta(0) - \eta_\infty} = 3 \frac{AC + BD}{C^2 + D^2}, \\ I(\omega) &\equiv \frac{\eta''(\omega)}{\eta(0) - \eta_\infty} = 3 \frac{AD - BC}{C^2 + D^2}. \end{aligned} \quad (3.17)$$

In Fig. 1 we plot these functions versus $\log_{10} \hat{\omega}$. The functions vary over a remarkably wide frequency range. The imaginary part $I(\omega)$ takes its maximum value 0.3025 at $\hat{\omega}_{\max} = 5.8269$. At this point $R(\omega)$ takes the value 0.5957.

In Fig. 2 we plot $\log_{10} \hat{\omega} R(\hat{\omega})$ and $\log_{10} \hat{\omega} I(\hat{\omega})$ versus $\log_{10} \hat{\omega}$. These functions are related to the dynamic shear modulus by Eq. (2.2). Plots of this type are familiar from the theory of polymer solutions.^{1,8}

In Fig. 3 we plot the real and imaginary parts of the radial function $f(x, \omega)$ at a frequency corresponding to $\hat{\omega}_{\max} = 5.8269$. For comparison, we also plot the radial function at zero frequency given by $f(x, 0) = 4/3x^3$.

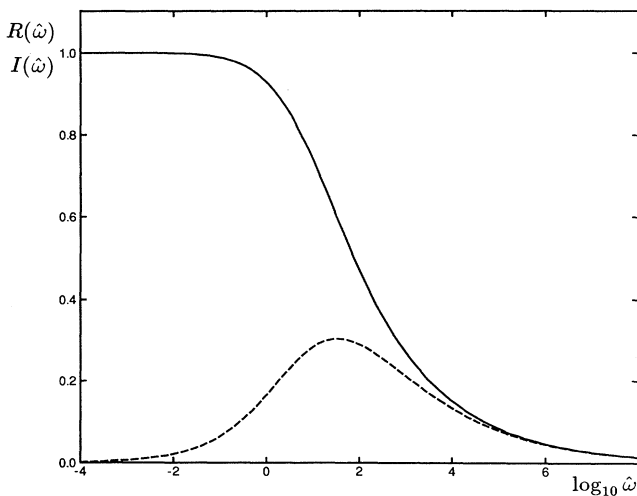


FIG. 1. Plot of the reduced functions $R(\hat{\omega})$ (drawn curve) and $I(\hat{\omega})$ (dashed curve) as given by (3.17).

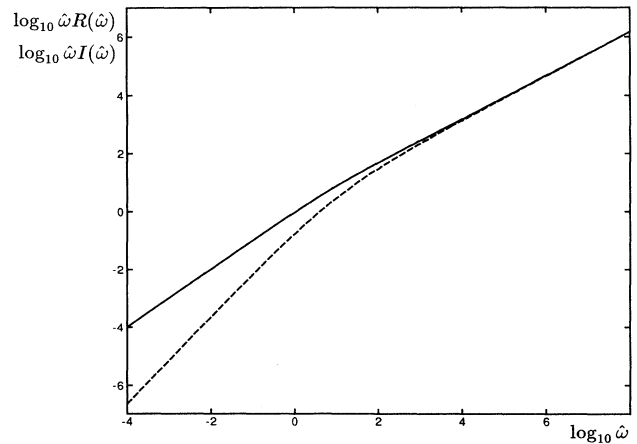


FIG. 2. Plot of $\log_{10} \hat{\omega} R(\hat{\omega})$ (drawn curve) and $\log_{10} \hat{\omega} I(\hat{\omega})$ (dashed curve) as given by (3.17).

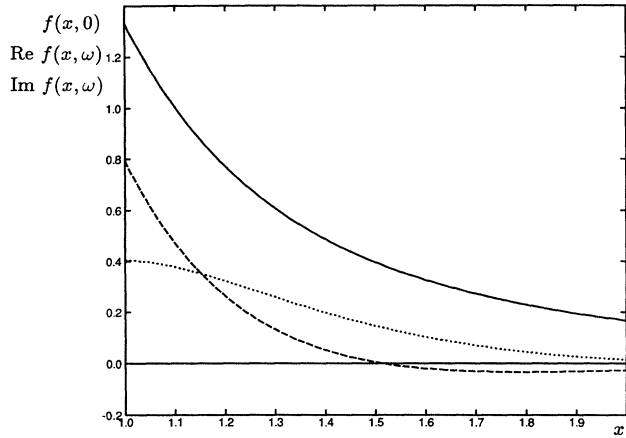


FIG. 3. Plot of the real and imaginary parts of the radial function $f(x, \omega)$ at frequency $\hat{\omega} = 5.8269$ (real part, dashed curve; imaginary part, dotted curve). We also plot $f(x, 0) = 4/3x^3$ (drawn curve).

IV. SPECTRUM AND RELAXATION FUNCTION

In this section we investigate the spectral density and the relaxation function corresponding to the dynamic viscosity given by (3.2) and (3.9). We may perform an analytic continuation by assuming (3.2) and (3.9) together with (3.6) to be valid everywhere in the complex frequency plane, and choosing the square-root branch cut along the negative imaginary axis. This shows that the dynamic viscosity may be written in the form (2.15) with spectral density

$$p(u) = \frac{4u^{5/2}}{8u^3 - 8u^2 + 18u + 81} \tag{4.1}$$

One may verify this expression by considering the limit $\hat{\omega} = -i\gamma + \epsilon$, with γ positive and ϵ infinitesimal. For small u , the spectral density behaves as

$$p(u) \approx \frac{4}{81} u^{5/2} \text{ as } u \rightarrow 0 \tag{4.2}$$

This determines the long-time behavior of the relaxation function. For large u ,

$$p(u) \approx \frac{1}{2} u^{-1/2} \text{ as } u \rightarrow \infty \tag{4.3}$$

This corresponds to the high-frequency behavior shown in (3.15) and also determines the short-time behavior of the relaxation function. In Fig. 4 we plot the spectral density $p(u)$.

In analogy to (2.13), the relaxation function is given by

$$\Psi(t) = \frac{G_v \tau_0}{\eta} \int_0^\infty p(u) \exp\left[\frac{-ut}{\tau_0}\right] du \tag{4.4}$$

By use of (3.16), (4.3), and a theorem on Laplace transforms,¹⁴ we hence find that $\Psi(t)$ has the short-time behavior

$$\Psi(t) \approx \frac{18}{5} \left[\frac{2}{\pi}\right]^{1/2} \phi^2 \left[\frac{\tau_0}{t}\right]^{1/2} \text{ as } t \rightarrow 0 \tag{4.5}$$

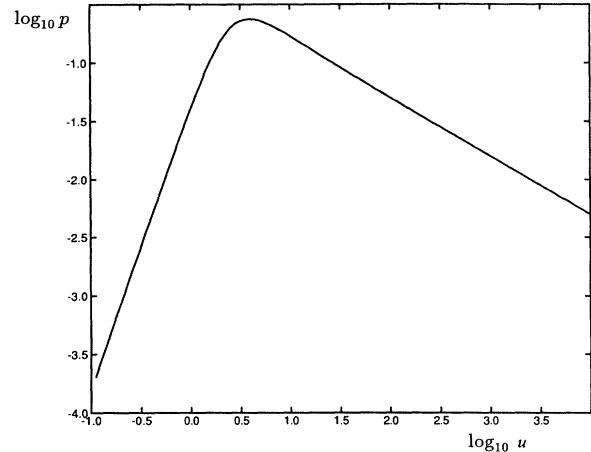


FIG. 4. Plot of the spectral density $p(u)$, as given by (4.1).

By use of (3.16) and (4.1), we find the complete expression

$$\Psi(t) = \frac{144\sqrt{2}}{5\pi} \phi^2 \int_0^\infty \frac{u^{5/2}}{8u^3 - 8u^2 + 18u + 81} \times \exp\left[\frac{-ut}{\tau_0}\right] du \tag{4.6}$$

This may be written as

$$\Psi(t) = \frac{18\sqrt{2}}{5\pi} \phi^2 \psi(t/\tau_0) \tag{4.7}$$

with the function

$$\psi(s) = \int_{-\infty}^\infty \frac{8x^6}{8x^6 - 8x^4 + 18x^2 + 81} e^{-sx^2} dx \tag{4.8}$$

Separating into partial fractions, we obtain

$$\psi(s) = \left[\frac{\pi}{s}\right]^{1/2} - \int_{-\infty}^\infty \left[\frac{A_0}{x^2 - u_0} + \frac{A_1}{x^2 - u_1} + \frac{A_2}{x^2 - u_2}\right] e^{-sx^2} dx \tag{4.9}$$

where u_0, u_1 , and u_2 are the roots of the cubic equation

$$u^3 - u^2 + \frac{9}{4}u + \frac{81}{8} = 0 \tag{4.10}$$

and the amplitudes A_0, A_1 , and A_2 satisfy

$$\begin{aligned} A_0 + A_1 + A_2 &= -(u_0 + u_1 + u_2) = -1, \\ (u_1 + u_2)A_0 + (u_2 + u_0)A_1 + (u_0 + u_1)A_2 &= -(u_0u_1 + u_1u_2 + u_2u_0) = -\frac{9}{4}, \\ u_1u_2A_0 + u_2u_0A_1 + u_0u_1A_2 &= -u_0u_1u_2 = \frac{81}{8}. \end{aligned} \tag{4.11}$$

Solving for the amplitudes, one finds

$$\begin{aligned} A_0 &= \frac{u_0^3}{(u_0 - u_1)(u_2 - u_0)}, \quad A_1 = \frac{u_1^3}{(u_1 - u_2)(u_0 - u_1)}, \\ A_2 &= \frac{u_2^3}{(u_2 - u_0)(u_1 - u_2)}. \end{aligned} \tag{4.12}$$

The roots are given by

$$\begin{aligned} u_0 &= -1.58998, \quad u_1 = u'_1 + iu''_1, \quad u_2 = u_1^*, \\ u'_1 &= 1.29499, \quad u''_1 = 2.16587. \end{aligned} \quad (4.13)$$

The first term in (4.9) yields the short-time behavior found already in (4.5). The integrals in (4.9) may be expressed in terms of the complementary error function. We find

$$\begin{aligned} \psi(s) &= \left[\frac{\pi}{s} \right]^{1/2} - \frac{\pi A_0}{\sqrt{|u_0|}} w(i\sqrt{|u_0|}s) \\ &+ 2\pi \text{Im} \frac{A_1}{\sqrt{u_1}} w(\sqrt{u_1}s), \end{aligned} \quad (4.14)$$

where

$$w(z) = e^{-z^2} \text{erfc}(-iz). \quad (4.15)$$

In the last term in (4.14), the square roots are taken to have a positive imaginary part. The frequency $\psi(s)$ was also encountered in the theory of self-diffusion.¹⁵ We plot the function $\psi(s)$ in Fig. 5.

The long-time behavior of $\Psi(t)$ is obtained most easily by use of the expression

$$\int_0^\infty e^{i\omega t} \Psi(t) dt = \phi^2 \tau_0 \alpha_V(\omega) \quad (4.16)$$

and a second theorem on Laplace transforms.¹⁶ From (3.9) we find for small ω

$$\alpha_V(\omega) = \frac{12}{5} \left[1 + \frac{2}{9} i\hat{\omega} - \frac{16}{81} \hat{\omega}^2 - \frac{4\sqrt{2}}{27} i\hat{\omega}^{5/2} + O(\hat{\omega}^3) \right]. \quad (4.17)$$

Hence we find that the long-time behavior of the relaxation function is given by

$$\Psi(t) \approx \frac{2\sqrt{2}}{3\sqrt{\pi}} \phi^2 \left[\frac{\tau_0}{t} \right]^{7/2}. \quad (4.18)$$

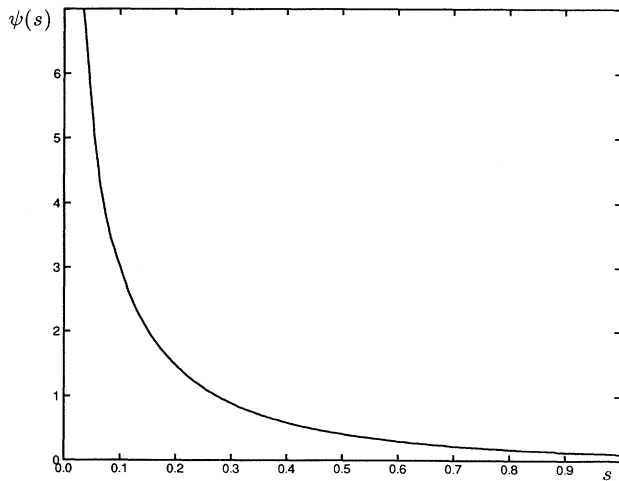


FIG. 5. Plot of the function $\psi(s)$ defined in (4.8). This is related to the stress-relaxation function by (4.7).

This is to be compared with the long-time tail of the stress-relaxation function in dense liquids found in molecular-dynamics simulations.¹⁷ In that case, the long-time tail decays as $t^{-3/2}$, and has an amplitude much larger than that predicted by mode-coupling theory.¹⁸ For interacting Brownian particles, Hess and Klein¹⁹ have predicted a $t^{-7/2}$ tail from mode-coupling theory.

The relaxation function shows quite remarkable behavior, both at short and at long times. As we have shown, the spectral density has corresponding features at large and small relaxation rates.

V. EXCLUDED SHELL

So far we have neglected direct interactions besides the hard-sphere repulsion. In experimental systems, direct interactions are often important. In particular, in suspensions of charged polystyrene spheres, the particles experience a strong repulsive interaction with a range of the order of the Debye length. In this section we consider a simple model in which the direct interaction is approximated by a hard-sphere repulsion at a radius b larger than the hydrodynamic radius a . It is fairly easy to see that the dynamic behavior is essentially the same as for $b=a$, but evolves on the longer time scale $\tau_1 = (b^2/a^2)\tau_0 = b^2/D_0$.

It follows from the linear-response theory that the dimensionless coefficient $\alpha_V(\omega)$ in (3.2) is now given by

$$\alpha_V(\omega) = \frac{9}{5} x_1^3 f(x_1, \omega), \quad (5.1)$$

where $x_1 = b/a$ is the ratio of radii. The radial function $f(x, \omega)$ again satisfies the differential equation (3.5), but now with the boundary condition $f'(x_1) = -4x_1$. Hence, instead of (3.8), we find

$$f(x, \omega) = -\frac{4x_1}{\alpha k'_2(\alpha x_1)} k_2(\alpha x), \quad (5.2)$$

and (3.9) is modified to

$$\alpha_V(\omega) = \frac{36}{5} x_1^5 \frac{(\alpha x_1)^2 + 3\alpha x_1 + 3}{(\alpha x_1)^3 + 4(\alpha x_1)^2 + 9\alpha x_1 + 9}. \quad (5.3)$$

In particular, at zero frequency,

$$\eta(0) = \eta_\infty + \frac{12}{5} x_1^5 \phi^2 \eta, \quad (5.4)$$

a result found earlier by Russel.¹³ By comparison with (3.6) we verify the time scaling mentioned above. The high-frequency behavior of the viscosity is given by

$$\begin{aligned} \eta'(\omega) &\approx \eta_\infty + \frac{18}{5} x_1^4 \frac{\phi^2}{\sqrt{\omega\tau_0}} \eta, \\ \eta''(\omega) &\approx \frac{18}{5} x_1^4 \frac{\phi^2}{\sqrt{\omega\tau_0}} \eta \quad \text{as } \omega \rightarrow \infty. \end{aligned} \quad (5.5)$$

From (5.4) and (5.5) one finds for the relaxation strength

$$G_v = \frac{36\sqrt{2}}{5\pi} x_1^3 \frac{\phi^2}{\tau_0} \eta. \quad (5.6)$$

The scaling of the remaining quantities is easily deduced.

VI. COMPARISON WITH EXPERIMENT

The theoretical results found above appear to be closely related to a recent experiment by van der Werff *et al.*⁴ Unfortunately, at the present time it is difficult to do experiments at volume fractions less than 0.1. The experimental data have been taken for concentrated suspensions with volume fractions between 0.3 and 0.6. Nonetheless, there is a remarkable qualitative agreement with the results found above for semidilute suspensions. Van der Werff *et al.* find that the real and imaginary parts of the dynamic viscosity show $\omega^{-1/2}$ behavior over a wide frequency range. The authors have analyzed their data in terms of a discrete relaxation spectrum, for which $\eta'(\omega)$ and $\eta''(\omega)$ take the form

$$\eta'(\omega) = \eta_\infty + G_1 \sum_{j=1}^N \frac{j^2 \tau_1}{j^4 + \omega^2 \tau_1^2}, \quad (6.1)$$

$$\eta''(\omega) = G_1 \sum_{j=1}^N \frac{\omega \tau_1^2}{j^4 + \omega^2 \tau_1^2},$$

with N large. For the Rouse model of dilute polymer solutions, the dynamic viscosity takes the same form.⁵ At large frequencies, (6.1) may be approximated by

$$\eta'(\omega) \approx \eta_\infty + \frac{\pi}{2\sqrt{2}} G_1 \tau_1^{1/2} \omega^{-1/2}, \quad (6.2)$$

$$\eta''(\omega) \approx \frac{\pi}{2\sqrt{2}} G_1 \tau_1^{1/2} \omega^{-1/2},$$

which is of the form (3.15). By comparison with (2.16), we find the relaxation strength

$$G_v = (\tau_1/\tau_0)^{1/2} G_1. \quad (6.3)$$

The discrete spectrum is somewhat unrealistic for hard-sphere suspensions, and we shall use instead the continuous density

$$p(u) = \frac{1}{2} u^{-1/2} \Theta(u - u_1), \quad (6.4)$$

with $u_1 = \sqrt{\tau_0/\tau_1}$. This corresponds to the dynamic viscosity

$$\eta(\omega) = \eta_\infty + \frac{1}{2} G_1 \tau_1 \int_{u_1}^{\infty} \frac{\sqrt{u_1}}{\sqrt{u} (u - z)} du. \quad (6.5)$$

Hence we find for the real and imaginary parts

$$\eta'(\omega) = \eta_\infty + \frac{1}{2} G_1 \tau_1 \left[K \left[\frac{\hat{\omega}}{u_1} \right] + L \left[\frac{\hat{\omega}}{u_1} \right] \right], \quad (6.6)$$

$$\eta''(\omega) = \frac{1}{2} G_1 \tau_1 \left[K \left[\frac{\hat{\omega}}{u_1} \right] - L \left[\frac{\hat{\omega}}{u_1} \right] \right],$$

with the functions

$$K(x) = \frac{1}{\sqrt{2x}} \arctan \frac{\sqrt{2x}}{1-x}, \quad (6.7)$$

$$L(x) = \frac{1}{\sqrt{2x}} \ln \frac{(1+x^2)^{1/2}}{1-\sqrt{2x}+x}.$$

These functions have the properties

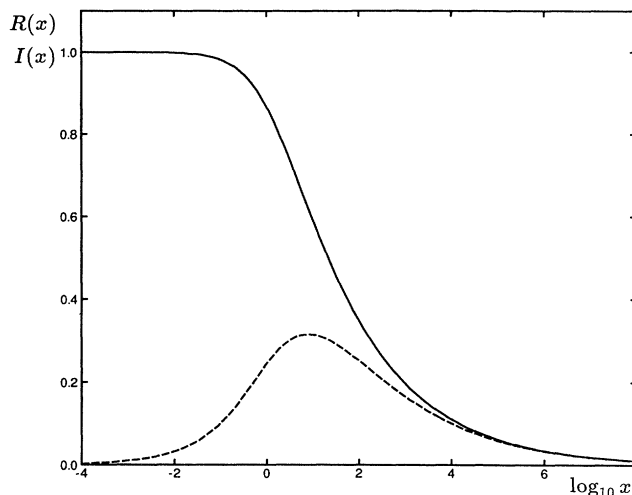


FIG. 6. Plot of the reduced functions $R(x)$ (drawn curve) and $I(x)$ (dashed curve) as given by (6.9).

$$\begin{aligned} K(0) &= 1, \quad L(0) = 1, \\ K(x) &\approx \frac{\pi}{\sqrt{2x}}, \quad L(x) \approx \frac{1}{x} \quad \text{as } x \rightarrow \infty. \end{aligned} \quad (6.8)$$

Clearly, the frequency dependence scales with τ_1 . In Fig. 6 we plot the scaling functions

$$\begin{aligned} R(x) &= \frac{1}{2} [K(x) + L(x)], \\ I(x) &= \frac{1}{2} [K(x) - L(x)]. \end{aligned} \quad (6.9)$$

The function $I(x)$ takes its maximum value 0.3152 at $x_{\max} = 2.8182$. At this point $R(x_{\max}) = 0.6218$. There is a remarkable similarity with Fig. 1. If we determine the relaxation time τ_1 by equating

$$\eta(0) = \eta_\infty + G_1 \tau_1 \quad (6.10)$$

with $\eta_\infty + (12/5)\eta\phi^2$ and using (3.16) and (6.3) we find $\tau_1 = (\pi^2/18)\tau_0$. For this relaxation time the reduced functions defined in (3.17) practically coincide with those found from (6.6).

Van der Werff *et al.*⁴ have determined the relaxation strength G_1 and the relaxation time τ_1 by fitting the experimental data with the expressions (6.1). Alternatively, one could fit with the expressions (6.6) arising from the more plausible spectral density (6.4). From the discussion above, it follows that one could equally well use the spectral density (4.1) of the dilute system and scale with the two parameters G_1 and τ_1 . Conversely, we conclude that the diffusion mechanism studied in the theory of semidilute suspensions may be held responsible for the $\omega^{-1/2}$ behavior observed in the dynamic viscosity of dense suspensions. We recall that the $\omega^{-1/2}$ behavior of the dynamic viscosity at high frequency corresponds to $t^{-1/2}$ behavior of the stress-relaxation function at short times.

VII. DISCUSSION

We have shown that the dynamic viscosity of hard-sphere suspensions may be calculated exactly to second order in the volume fraction if hydrodynamic interactions and direct interactions in addition to the hard-sphere repulsion are neglected. The dynamic viscosity shows an interesting $\omega^{-1/2}$ behavior at high frequency, in agreement with experimental data on dense suspensions.

It will be of great interest to investigate the influence of hydrodynamic and direct interactions. We have shown that for an excluded shell potential, the dynamic viscosity may be obtained by scaling from the hard-sphere model.

In future work we intend to study a wider class of direct interactions. It has been shown by Russel and Gast²⁰ that the dynamic viscosity decays in proportion to ω^{-1} at high frequency if hydrodynamic interactions are included. This does not exclude the possibility that the viscosity exhibits $\omega^{-1/2}$ behavior in a wide frequency range. To settle this question, a more elaborate analysis is required.

ACKNOWLEDGMENTS

We thank the Deutsche Forschungsgemeinschaft for financial support.

*Also at Institute of Fundamental Technological Research, Polish Academy of Sciences, Świątokrzyska 21, 00-049 Warsaw, Poland.

¹J. D. Ferry, *Viscoelastic Properties of Polymers* (Wiley, New York, 1961).

²A. Einstein, *Ann. Phys.* **19**, 289 (1906); **34**, 591 (1911).

³G. K. Batchelor, *J. Fluid Mech.* **83**, 97 (1977).

⁴J. C. van der Werff, C. G. de Kruif, C. Blom, and J. Mellema, *Phys. Rev. A* **39**, 795 (1989).

⁵M. Doi and S. F. Edwards, *The Theory of Polymer Dynamics* (Clarendon, Oxford, 1986), p. 115.

⁶J. Mellema, C. G. de Kruif, C. Blom, and A. Vrij, *Rheol. Acta* **26**, 40 (1987).

⁷B. Gross, *Mathematical Structure of the Theories of Viscoelasticity* (Hermann, Paris, 1953).

⁸H. Yamakawa, *Modern Theory of Polymer Solutions* (Harper and Row, New York, 1971).

⁹See the review by P. N. Pusey and R. J. A. Tough, in *Dynamic*

Light Scattering and Velocimetry: Applications of Photon Correlation Spectroscopy, edited by R. Pecora (Plenum, New York, 1981).

¹⁰B. U. Felderhof and R. B. Jones, *Physica A* **146**, 417 (1987).

¹¹B. U. Felderhof, *Physica A* **147**, 533 (1988).

¹²B. Cichocki and B. U. Felderhof, *J. Chem. Phys.* **93**, 4427 (1990).

¹³W. B. Russel, D. A. Saville, and W. R. Schowalter, *Colloidal Dispersions* (Cambridge University, Cambridge, 1989), p. 499.

¹⁴G. Doetsch, *Einführung in Theorie und Anwendung der Laplace-Transformation* (Birkhäuser, Basel, 1958), p. 226.

¹⁵B. Cichocki and R. B. Jones, *Z. Phys. B* **68**, 513 (1987).

¹⁶Reference 14, p. 238.

¹⁷J. J. Erpenbeck and W. W. Wood, *J. Stat. Phys.* **24**, 455 (1981).

¹⁸J. P. Hansen and I. R. McDonald, *Theory of Simple Liquids* (Academic, London, 1986), p. 271.

¹⁹W. Hess and R. Klein, *Adv. Phys.* **32**, 173 (1983).

²⁰W. B. Russel and A. P. Gast, *J. Chem. Phys.* **84**, 1815 (1986).